Received: 28 February 2021 | Revised: 14 March 2021 | Accepted: 19 March 2021

DOI: 10.1111/trf.16393

ORIGINAL RESEARCH

TRANSFUSION

Purification and analysis of a protein cocktail capable of scavenging cell-free hemoglobin, heme, and iron

Ivan S. Pires[1] | **Krianthan Govender**[2] | **Carlos J. Munoz**[2] | **Alexander T. Williams**[2] | **Quintin T. O'Boyle**[1] | **Chintan Savla**[1] | **Pedro Cabrales**[2] | **Andre F. Palmer**[1]

[1]William G. Lowrie Department of Chemical and Biomolecular Engineering, The Ohio State University, Columbus, Ohio, USA

[2]Department of Bioengineering, University of California San Diego, La Jolla, California, USA

Correspondence
Andre F. Palmer, William G. Lowrie Department of Chemical and Biomolecular Engineering, The Ohio State University, 452 CBEC, 151 West Woodruff Ave, Columbus, OH 43210, USA.
Email: palmer.351@osu.edu

Funding information
National Cancer Institute, Grant/Award Number: P30 CA016058; National Heart, Lung, and Blood Institute, Grant/Award Numbers: R01HL126945, R01HL138116; National Institute of Biomedical Imaging and Bioengineering, Grant/Award Number: R01EB021926; NIH Office of the Director, Grant/Award Number: S10 OD018056; Ohio State University Comprehensive Cancer Center - Arthur G. James Cancer Hospital and Richard J. Solove Research Institute, Grant/Award Number: Pelotonia Fellowship Program; The Ohio State University Office of Undergraduate Research & Creative Inquiry, Grant/Award Number: Summer Research Fellowship

Abstract

Background: Hemolysis releases toxic cell-free hemoglobin (Hb), heme, and iron, which overwhelm their natural scavenging mechanisms during acute or chronic hemolytic conditions. This study describes a novel strategy to purify a protein cocktail containing a comprehensive set of scavenger proteins for potential treatment of hemolysis byproducts.

Study Design and Methods: Tangential flow filtration was used to purify a protein cocktail from Human Cohn Fraction IV (FIV). A series of in vitro assays were performed to characterize composition and biocompatibility. The in vivo potential for hemolysis byproduct mitigation was assessed in a hamster exchange transfusion model using mechanically hemolyzed blood plasma mixed with the protein cocktail or a control colloid (dextran 70 kDa).

Results: A basis of 500 g of FIV yielded 62 ± 9 g of a protein mixture at 170 g/L, which bound to approximately 0.6 mM Hb, 1.2 mM heme, and 1.2 mM iron. This protein cocktail was shown to be biocompatible in vitro with red blood cells and platelets and exhibits nonlinear concentration dependence with respect to viscosity and colloidal osmotic pressure. In vivo assessment of the protein cocktail demonstrated higher iron transport to the liver and spleen and less to the kidney and heart with significantly reduced renal and cardiac inflammation markers and lower kidney and hepatic damage compared to a control colloid.

Discussion: Taken together, this study provides an effective method for large-scale production of a protein cocktail suitable for comprehensive reduction of hemolysis-induced toxicity.

KEYWORDS

heme, hemoglobin, hemolysis, iron, protein scavenger, red blood cells, tangential flow filtration

1 | INTRODUCTION

Red blood cell (RBC) lysis, a phenomenon referred to as hemolysis, results in circulating cell-free hemoglobin (Hb), heme, and iron.[1] Intravascularly, cell-free Hb extravasates through the blood vessel wall into the interstitial tissue space and scavenges nitric oxide (NO), eliciting vasoconstriction and systemic

hypertension.[2] As natural mechanisms to remove Hb are limited, cell-free Hb elicits oxidative damage to proteins, lipids, nucleic acids, and other macromolecules.[3] Free heme is involved in various vascular pathologies and, due to its hydrophobicity, avidly binds to lipid surfaces or plasma proteins, mediating their oxidation.[2,4] Lastly, iron also causes oxidative damage through generation of reactive oxygen species.[5–7] Hence, hemolysis above the natural capacity to detoxify Hb can lead to vasoconstriction, hypertension, vascular disease, inflammation, thrombosis, hemoglobinuria, and renal damage.[2,8]

Unfortunately, many clinical conditions are associated with acute or chronic hemolysis, but there are no approved treatments to attenuate hemolysis-mediated toxicity.[2,9] In preclinical studies, hemolysis treatment strategies have focused on single protein supplementation therapies consisting of either haptoglobin (Hp), hemopexin (Hpx), or transferrin (Tf), which bind to Hb, heme, and iron, respectively.[1,10] For example, the Hb scavenging protein Hp has been shown to improve shock, lung injury, and survival in canine pneumonia models.[11] Hp has also been shown to reduce acute kidney injury (AKI) in animal models and humans following massive blood transfusions.[2] Furthermore, the toxicity from stored RBCs may be attenuated with Hp, Hpx, or Tf.[12,13] Although promising results have been obtained with single-agent plasma protein supplementation, hemolysis is a multifaceted disease state with a milieu consisting of cell-free Hb, heme, and iron contributing to its overall toxicity.[14–17] Therefore, a mixture of the therapeutic plasma proteins (Hp, Hpx, and Tf) could yield improved outcomes during hemolytic disease states.

In a previous study, we demonstrated the purification of Hp via tangential flow filtration (TFF) of Human Cohn Fraction IV (FIV) using a series of hollow fiber filters to bracket the plasma proteins based on their molecular weight (MW).[18] The key advantages of this process are that TFF is an easily scalable separation method and FIV is a waste product from the plasma fractioning industry, making the Hp purification process cost-effective and amenable for large-scale Hp production. Interestingly, based on the composition of FIV, the last permeate fraction from the TFF Hp purification process may serve as a source of the therapeutic proteins required for comprehensive hemolysis treatment.[18] In this study, the last permeate of the TFF Hp purification process was retained on a 50 kDa hollow fiber (HF) filter, and the isolated product was characterized to develop a cost-effective and simple protein cocktail for potential treatment of hemolysis.

2 | MATERIALS AND METHODS

2.1 | Materials

Sodium phosphate dibasic, sodium phosphate monobasic, sodium chloride, and fumed silica (S5130) were purchased (Sigma Aldrich, St. Louis, MO), and 0.2 μm polyethersulfone syringe filters were also purchased (Merck Millipore, Billerica, MA). Protein separation was performed on a TFF system (KrosFlo® Research II, Repligen, Waltham, MA). The TFF system was equipped with various HF filter modules (Repligen, Waltham, MA). FIV paste from the modified Cohn process of Kistler and Nitschmann was purchased (Seraplex, Inc., Pasadena, CA).

2.2 | Hb, heme, and iron scavenging protein cocktail purification via TFF

Purification of the protein cocktail followed the TFF Hp purification method with the addition of one additional TFF stage at the end of the original process.[18] Briefly, 500 g of FIV was suspended in 5 L of phosphate-buffered saline (PBS) and homogenized in a blender. After stirring overnight at 4°C, approximately 5 L of the solution was centrifuged to remove undissolved lipids. Fumed silica was then added to the supernatant to remove lipids and lipoproteins, left to stir overnight at 4°C, and then recentrifuged with two PBS washes of the fumed silica pellet. The resulting protein solution was then clarified on a 0.2 μm HF filter and then bracketed using a series of HF modules with decreasing MW cutoff (MWCO) (750, 500, and 100 kDa). Unlike the base TFF Hp purification process, the permeate of the 100 kDa HF filter (Stage 3) was retained on a 50 kDa HF module (P/N: S02-E100-05-N). The new bracket (Stage 4) was subject to constant volume diafiltration with 5× volume PBS and finally concentrated to approximately 350 ml. A diagram of the entire purification process is shown in Figure 1.

2.3 | HPLC-size exclusion chromatography (SEC)

Samples from the purification process were separated via HPLC-SEC using a commercial column (4.6 × 300 mm Acclaim SEC-1000, Thermo Fisher Scientific, Waltham, MA) attached to an HPLC system (Dionex UltiMate 3000, Thermo Fisher Scientific, Waltham, MA) as described previously in the literature.[18]

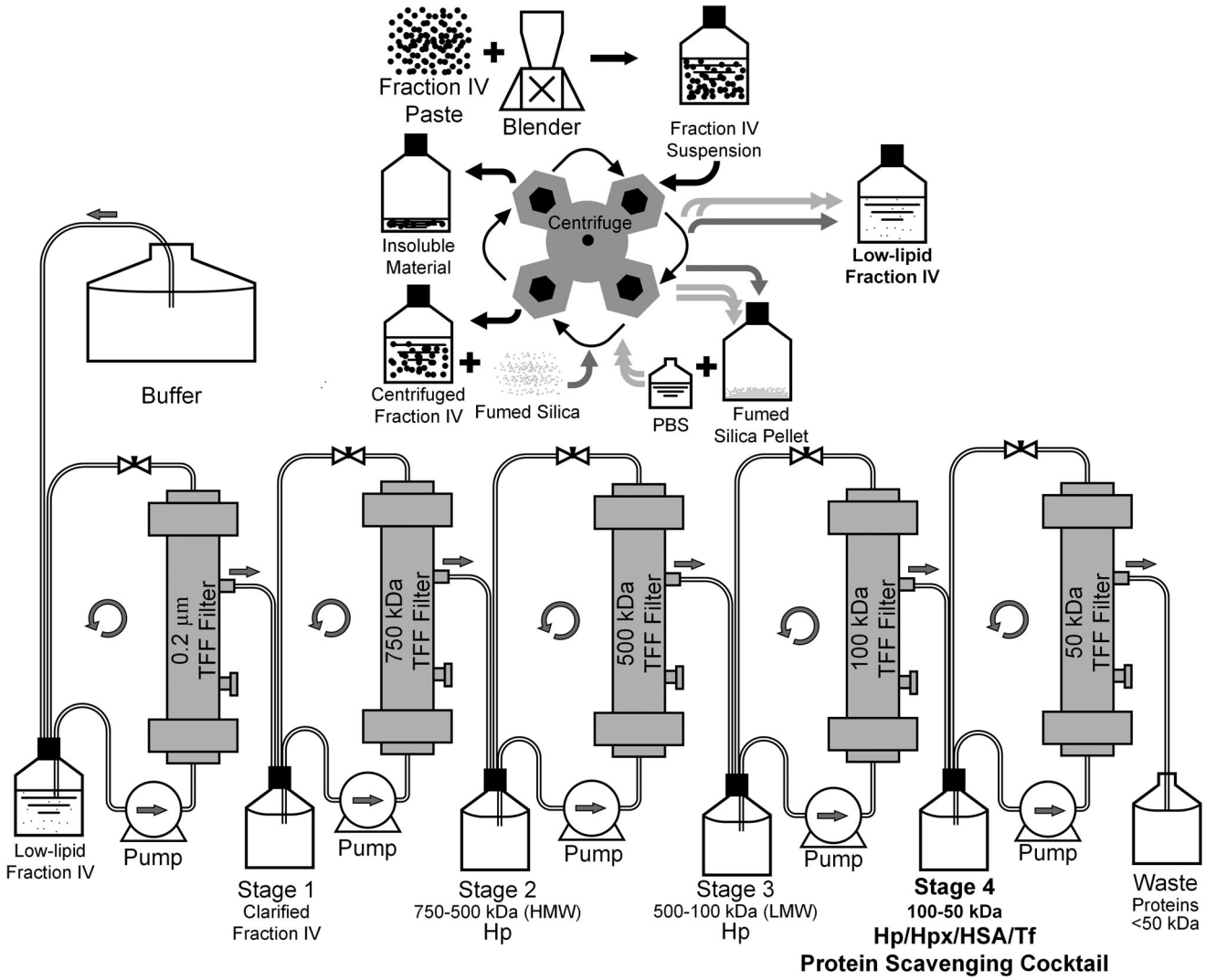

FIGURE 1 Overview of the process used to purify both Hp (Stages 2 and 3), and the Hb, heme, and iron scavenging protein cocktail (Stage 4). HMW, high MW fraction; LMW, low MW fraction. Arrows indicate the direction of flow in the circuit. Figure adapted with permission from reference 18. Copyright 2020, John Wiley and Sons

2.4 | Hb concentration

The concentration of Hb in the samples was measured spectrophotometrically via the Winterbourn equations.[19]

2.5 | Gel electrophoresis

The purity and composition of the protein cocktail were analyzed via SDS-PAGE using commercial equipment (Invitrogen Mini Gel Tank, Thermo Fisher Scientific, Waltham, MA). The samples were prepared according to the manufacturer's guidelines and as previously described.[18,20]

2.6 | Total protein assay

Total protein was determined via the Bradford assay.

2.7 | Hb binding capacity of Hp

The difference in MW between the Hp–Hb protein complex and pure Hb was used to assess the Hb binding capacity (HbBC) of Hp using HPLC-SEC as previously described.[18] Briefly, the samples containing Hp were mixed with excess Hb and then separated via HPLC-SEC. The difference in the area under the curve (AUC) between the pure Hb solution and the mixture of Hb and

Hp was used to assess the HbBC of Hp. A representative HPLC-SEC chromatogram of this assay is shown in Figure S1(A).

2.8 | Iron binding activity

The iron-binding capacity (FeBC) of Tf contained in the protein scavenger cocktail was determined via reaction with ferric nitrilotriacetate [Fe(NTA)]. Briefly, the Tf sample was reacted with excess Fe(NTA), and the equilibrium change in absorbance was measured (Figure S1(B)). The extinction coefficient of holo-Tf at 465 nm was then used to estimate the concentration of iron bound to Tf (FeBC).[21] The holo-Tf concentration was determined based on the 465 nm absorbance of the sample prior to the addition of Fe(NTA) (contribution of residual metHb in the sample at 465 nm was estimated based on the sample absorbance at 404 nm[22]).

2.9 | Heme binding activity

The heme-binding capacity (HemeBC) in the purified protein scavenger cocktail was determined via the dicyanohemin (DCNh) incorporation assay.[23] Briefly, the sample was mixed with increasing concentrations of DCNh, and the equilibrium absorbance of the Soret peak maxima was measured. The inflection point in the graph of the equilibrium absorbance versus DCNh concentration was used to determine the saturation point of the heme-binding pockets (Figure S1(C))). To determine the heme-binding activity of Hpx individually, the protein cocktail was mixed with excess heme-bound HSA (hHSA) and the change in absorbance was used to determine the concentration of heme-Hpx (Figure S1(D)).[24]

2.10 | Trypsin digest mass spectrometry

Protein identification in the protein cocktail was confirmed using trypsin digest nano-liquid chromatography–nanospray tandem mass spectrometry (LC/MS/MS) on a commercial mass spectrometer (Fusion Orbitrap equipped with EASY-Spray™ Sources, Thermo Scientific, San Jose, CA) operated in positive ion mode as described previously in the literature.[18]

2.11 | MALDI-TOF-MS

The samples were diluted to 0.5 mg/ml on a protein basis in deionized water. The reduced samples were prepared by adding 0.1 M dithiothreitol to the protein samples. A saturated solution of α-cyano-4-hydroxycinnamic acid matrix was prepared in 50% v/v acetonitrile with 0.1% trifluoroacetic acid. A total of 1 μl of the mixture of the matrix and protein solution was deposited on a matrix-assisted laser desorption/ionization (MALDI) plate and analyzed on a MALDI-TOF (time of flight) MS (mass spectrometry) system (Microflex, Bruker, Billerica, MA).

2.12 | ELISA

The concentration of selected protein components in FIV and in the protein cocktail was quantified via ELISA kits specific for Hp, Tf, HSA, and Hpx according to the manufacturer's instructions (R&D Systems Catalog #DHAPG0 for Hp, and Eagle BioSciences HTF31-K01 for Tf, HUA39-K01 for HSA, and HPX39-K01 for Hpx).

2.13 | Viscosity and colloidal osmotic pressure (COP) measurements

The viscosity of 5% (w/v) HSA and the protein cocktail solution was measured using a cone/plate viscometer (DV-II plus with a cone spindle CPE-40, Brookfield Engineering Laboratories, Middleboro, MA) at a shear rate of 316 s^{-1}, whereas the COP was measured using a colloid osmometer (Wescor 4420, Logan, UT).

2.14 | RBC aggregation

The extent of RBC aggregation of fresh rat whole blood mixed with the test solutions (protein cocktail, saline, 500 kDa dextran, and 5% (w/v) HSA) was evaluated in this study. Blood samples were collected into heparinized vacutainers (BD, San Diego, CA) and mixed with 20% by volume of the test solutions. The degree of RBC aggregation was assessed using a photometric rheoscope (Myrenne Aggregometer, Myrenne, Roetgen, Germany) as previously described.[25,26]

2.15 | Coagulation studies

Coagulation studies were performed on platelets isolated from citrated (3.2% buffered trisodium citrate, Sigma-Aldrich) rat whole blood and mixed with the protein cocktail solution (20% by volume). Platelets were isolated and aggregation was assessed as previously described subject to stimulation with two agonists: adenosine diphosphate (ADP) and collagen.[27] The effect of the protein cocktail solution was compared to HSA (5% w/v) and Hextend (6% Hetastarch in Lactated Electrolyte

solution, Hospira) as control solutions in various platelet functional assays.

2.16 | Animal preparation

Animal handling and care followed the NIH Guide for the Care and Use of Laboratory Animals, and the experimental protocol was approved by the local animal care committee at the University of California San Diego. The studies were performed in 55–65 g male Golden Syrian Hamsters (Charles River Laboratories, Boston, MA) fitted with arterial and venous catheters. For catheter implantation, animals were re-anesthetized with ketamine/xylazine, and a PE-50 catheter with a PE-10 tip was implanted in the right carotid artery and in the jugular vein, secured with 5–0 silk sutures, exteriorized dorsally, and secured to the back of the animals. Hamsters were housed individually post-surgery and allowed to recover 1 or 2 days before subjected to the experiment.

2.17 | In vivo hamster exchange transfusion model

Hamster whole blood was adjusted to 40% hematocrit with 5% human serum albumin (HSA), and then mixed at 4:1 (volume ratio) with a 85 mg/ml solution of the protein cocktail or 6% dextran 70 kDa. A total of 5 ml of the resulting mixture was then mechanically hemolyzed in a sterile closed-loop heparin-coated silicone tube circuit with 0.8 mm inner tube diameter using a peristaltic pump running at 100 rpm (5 ml/min) for 12 h at room temperature. After mechanically hemolyzing the blood mixture, the plasma from the hemolyzed mixture was separated via centrifugation, and the supernatant was stored at −80°C. For in vivo testing, hemolyzed blood plasma filtered through a 0.2 μm filter was used to perform an isovolumic exchange transfusion of 5% of the animal's total Hb mass at a rate of 100 μl/min. Animals were euthanized for 2 h post-transfusion to collect the blood, liver, heart, spleen, and kidneys for analysis. Organ tissue was processed for inflammatory and organ damage markers as previously described[28] using the kits and assays outlined in Table S1.

2.18 | Statistical analysis

All data are represented as mean values ± SD. Data were compared using a one-way ANOVA with Tukey's multiple comparisons test for parametric data using commercial statistical software (GraphPad Prism 8.1, GraphPad Software Inc., San Diego, CA). Changes were considered significant if p values were less than .05.

3 | RESULTS

3.1 | Protein cocktail purification and composition

The results from three batches following the protein cocktail purification process outlined in Figure 1 are summarized in Table 1.

As shown in Table 1, each 500 g batch of FIV yielded more than 60 g of a concentrated protein cocktail composed primarily of HSA and Tf with approximately 10% and 5% of Hp and Hpx, respectively. ELISA results concurred with the activity binding assays, demonstrating that the proposed series of activity assays (Figure S1) was capable of accurately quantifying the different protein species in the sample.

To further analyze the composition of the protein cocktail, the samples were analyzed via SDS-PAGE, trypsin digest mass spectrometry (MS), and MALDI-TOF MS. The results of the representative samples are shown in Figure 2.

As expected, HSA, Tf, Hpx, and Hp were present in the SDS-PAGE (Figure 2(A) and (B)) and identified in the trypsin digest MS analysis (Figure 2(C)). The detection of haptoglobin-related protein (Hpr) was likely due to the high sequence identity of Hpr compared to the Hp1-1 phenotype.[18] Furthermore, ceruloplasmin (Cp) and vitamin-D binding protein (VDB) were also detected in the trypsin digest MS with similar ion intensities as Hpx. Thus, it would be expected that these components had similar mass composition to Hpx (approx. 5%).

Moreover, the various peaks in the MALDI-TOF MS spectra (Figure 2(D)) of the protein cocktail confirmed the presence of the expected protein species (see Supplemental Information for detailed MALDI-TOF MS analysis). Notably, MALDI-TOF MS data cannot be used as a quantitative method for assessment of composition as different proteins have different ionization efficiencies.[29] However, densitometric analysis of SDS-PAGE can provide quantitative insights into protein composition, and the results are shown in Table 2.

Densitometric analysis results agreed with the activity binding assay results where >90% of the protein cocktail was composed of four major proteins (HSA, Hpx, Hp, and Tf). Cp was also noticeable on the SDS-PAGE with approximately 4% mass composition. Hpx could only be partially estimated via SDS-PAGE analysis as it alters its apparent MW when reduced. Comparing the percent composition of Tf and the HSA band before and after

TABLE 1 Summary of the scavenging protein cocktail composition, concentration, and yield

	Total (g)	±	Concentration (mg/ml)	±	Yield (%)	±
Protein	61.9 (100%)	9.4	171	21	50	4
Hp[a]	5.97 (10%)	0.12	16.5 (16[b])	0.7	49	3
Hpx	2.21 (4%)	0.42	6.1 (8.8[b])	0.9	(52[b])	(2)
HSA[c]	28.7 (42%)	4.3	79.1 (75[b])	10.1	(88[b])	(10)
Total Tf[d]	21.2 (34%)	2.6	58.6 (63[b])	5.61	(81[b])	(9)
apoTf	18.2	2.7	50.1	6.03	-	-
Other	6.12 (10%)	2.4	16.9	6.1	-	-

	Concentration (mM)	±	Concentration (mg/ml)	±
HbBC	0.61	0.03	9.7	0.49
HemeBC	1.22	0.16	0.79	0.10
FeBC	1.25	0.15	0.070	0.008

Note: Percentage composition was assessed via the activity binding assays. All molar concentration values are provided on a globin/iron basis (i.e., tetrameric Hb contains four globin/iron equivalents, while both heme and iron contain one iron equivalent). Error is based on the standard deviation of three independent batches.

Abbreviations: FeBC, iron-binding capacity; HbBC, Hb-binding capacity; HemeBC, heme-binding capacity.

[a]Hp determined by assuming a 1:1.65 mass binding ratio of Hb:Hp2-2.

[b]Concentration and yield determined from ELISA kits.

[c]HSA determined by the total heme-binding capacity excluding the contribution from Hpx.

[d]Total Tf determined via summation of apoTf and holoTf which was derived from the non-Hb contribution from the absorbance at 460 nm.

reduction showed a 7%–9% change, indicating a similar composition as the estimation determined via the heme-binding assay (approx. 5%).

3.2 | Biophysical and biochemical properties of the protein cocktail

In vivo use of the protein cocktail requires understanding of the physicochemical properties of the mixture and its effects when administered into blood. Thus, the colloidal osmotic pressure (COP) and viscosity of the protein cocktail were assessed and compared to that of commercial 5% (w/v) HSA. The results are shown in Figure 3.

As shown in Figure 3, the protein cocktail had similar COP and viscosity to HSA at concentrations lower than 75 mg/ml. However, at high protein concentrations, both the COP and viscosity of the cocktail showed a nonlinear increase with protein concentration reaching values higher than pure HSA. Next, the protein cocktail was mixed with whole blood and platelet-rich plasma to assess its effects on RBC and platelet aggregation. The results are shown in Figure 4.

Based on the results shown in Figure 4(A) and (B), unlike 500 kDa dextran, the protein cocktail did not lead to RBC aggregation as its aggregation index was similar to that of blood mixed with saline or HSA. Furthermore, as shown in Figure 4(C) and (D), the collagen platelet aggregation test showed that the protein cocktail did not lead to significant platelet aggregation inhibition compared to the control or HSA. On the other hand, Hextend was the only material tested that significantly impaired platelet aggregation.

3.3 | In vivo efficacy of the protein cocktail at hemolysis treatment

The promising properties of the isolated protein cocktail in hemolysis treatment were tested in vivo by administering mechanically hemolyzed blood plasma mixed with either the protein cocktail or dextran 70 kDa (Dex70) via exchange transfusion at 5% of the animal's total Hb mass. Dex70 was chosen for comparison given its improved plasma expansion properties compared to HSA, potential anti-inflammatory effects, and interest as a pump-priming fluid.[30,31] Ferritin levels in the heart, kidney, liver, and blood were measured, and markers of tissue inflammation or injury were also assessed. As shown in Figure 5, 2 h post-exchange transfusion, there was a significantly altered iron distribution in the animals. Administration of the protein cocktail with hemolyzed blood plasma led to lower circulating levels of bilirubin and ferritin (Figure 5(A),(B)) in transfused animals. This

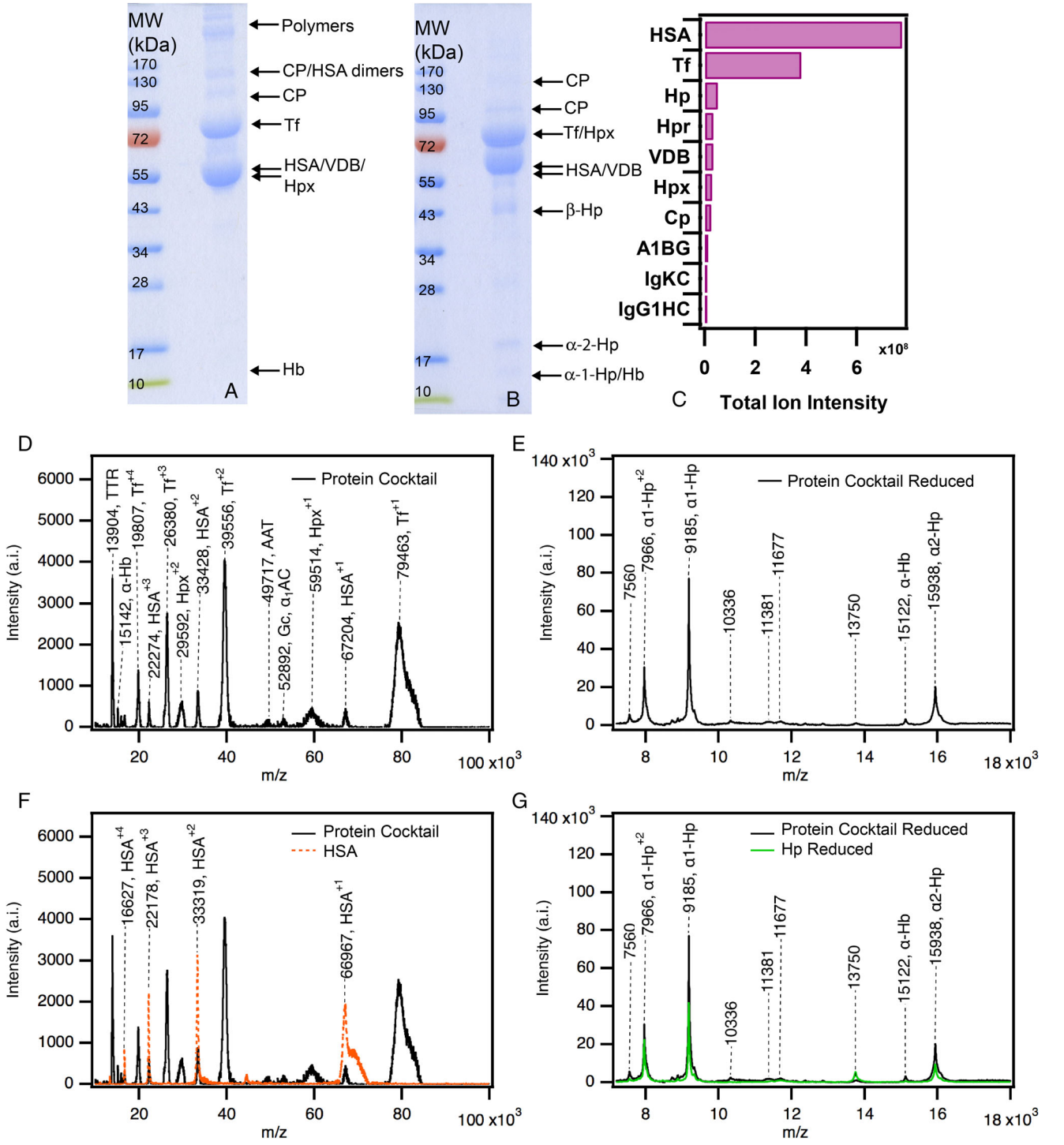

FIGURE 2 SDS-PAGE and mass spectrometry analysis of a representative batch of the scavenging protein cocktail. Images of the SDS-PAGE gel under nonreducing (A) and reducing (B) conditions. (C) Top 10 identified proteins from trypsin digest mass spectrometry of a representative batch of the scavenging protein cocktail. MALDI-TOF mass spectral analysis of the scavenging protein cocktail under (D) nonreducing and (E) reducing conditions. (F) Comparison of the scavenging protein cocktail with human serum albumin (HSA) under nonreducing conditions denoting the presence of common peaks in the two samples. (G) Comparison of the scavenging protein cocktail with haptoglobin 2–1, 2–2 mixture (Hp) under reducing conditions resulted in common peaks in the two species confirming the presence of Hp in the cocktail. Abbreviations: HSA, human serum albumin; Tf, transferrin; Hp, haptoglobin; Cp, ceruloplasmin; VDB, vitamin-D binding protein; Hpx, hemopexin; Hpr, haptoglobin-related protein; IgG1HC, immunoglobulin gamma 1 heavy chain; A1BG, α-1-B glycoprotein; IgkC, immunoglobulin kappa constant; TTR, transthyretin; AAT, α-1 antitrypsin; α1AC, α-1 antichymotrypsin; α-Hb, α chain hemoglobin; α1-Hp, α1 chain haptoglobin; α2-Hp, α2 chain haptoglobin [Color figure can be viewed at wileyonlinelibrary.com]

TABLE 2 Composition of the scavenging protein cocktail based on SDS-PAGE densitometric analysis

Non-reduced			Reduced		
Species	**Composition**	**+/−**	**Species**	**Composition**	**+/−**
HSA/Hpx/VDB	47.7%	1.7%	Tf/Hpx	42.4%	3.1%
Tf	31.2%	1.2%	HSA/VDB	40.3%	3.4%
Polymers (Hp)	15.2%	3.0%	β-Hp	4.8%	0.1%
Cp (135 kDa)	2.4%	0.0%	α-2Hp	3.3%	0.5%
HSA dimer/ Cp (115 kDa)	2.4%	0.1%	α-1Hp/Hb	3.0%	1.0%
Other	1.1%	0.0%	Cp (115 kDa)	1.9%	0.0%
			Other (>140 kDa)	1.7%	0.7%
			Cp (135 kDa)	1.7%	0.0%
			Other (~ kDa)	1.6%	0.4%
			β-2 glycoprotein	0.7%	0.1%

Note: Error is based on the standard deviation of three independent batches.
Abbreviations: Cp, ceruloplasmin; Hb, hemoglobin; Hp, haptoglobin; Hpx, hemopexin; HSA, human serum albumin; Tf, transferrin; VDB, vitamin-D binding protein (Gc-globulin).

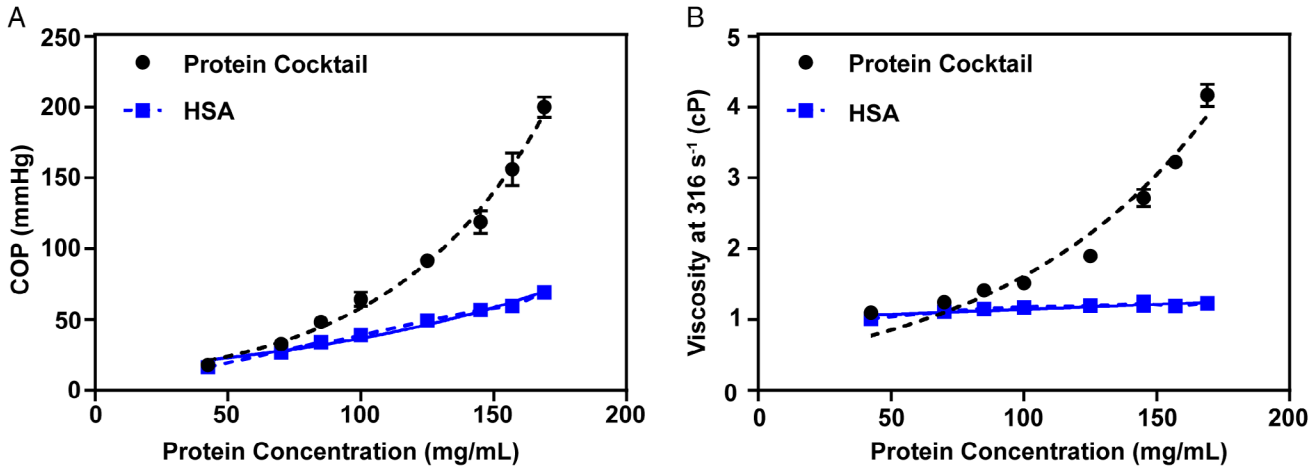

FIGURE 3 Physical properties of the protein cocktail. (A) Colloidal osmotic pressure (COP). (B) Viscosity measured at a shear rate of 316 s^{-1} [Color figure can be viewed at wileyonlinelibrary.com]

iron was directed to the proper clearance organs responsible for iron metabolism such as the spleen and liver (Figure 5(C),(D)) and prevented from accumulating in iron-sensitive organs such as the kidneys and heart (Figure 5(E),(F)). To further assess organ toxicity from transfusion of the hemolyzed blood plasma, inflammatory and injury markers for renal, hepatic, and cardiac tissues were measured and the results are shown in Figure 6.

As shown in Figures 6(A)–(O), inflammatory markers in renal, hepatic, and cardiac tissues were significantly reduced, approaching baseline levels in healthy animals. Notably, liver ferritin was elevated and the assayed markers of liver injury were reduced compared to Dex70, indicating detoxification of the iron-containing molecules released from hemolysis.

4 | DISCUSSION

Comprehensive treatment of hemolysis requires the scavenging of three toxic species: cell-free Hb, heme, and iron. Based on the results presented here, the isolated scavenging protein cocktail was capable of binding to these three molecules via Hp (approx. 10%), HSA (approx. 40%), Hpx (approx. 5%), and Tf (approx. 35%). Furthermore, the protein cocktail was also composed of Cp (approx. 5%) and VDB (approx. 5%), which can help

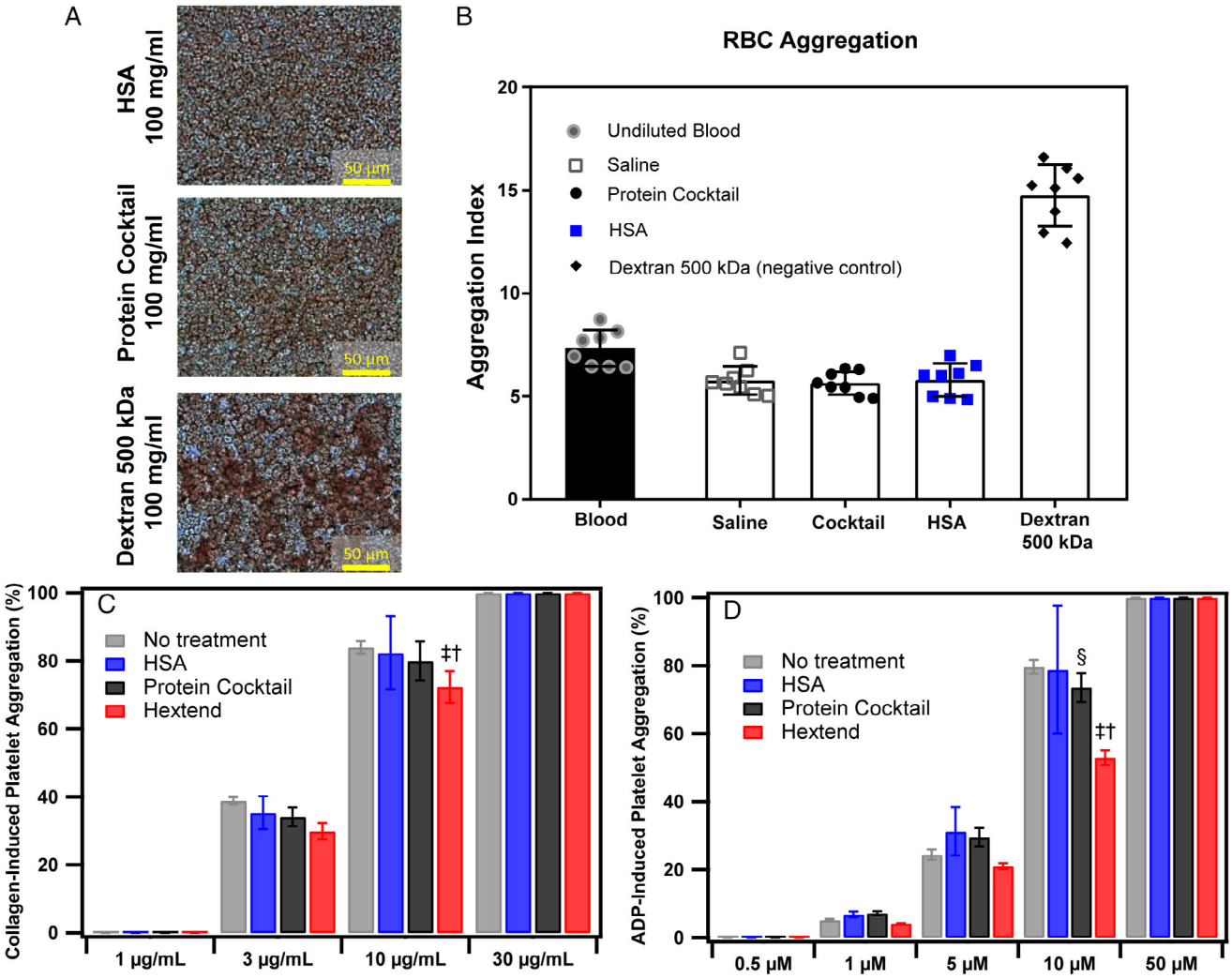

FIGURE 4 RBC aggregation and coagulation assays with the protein cocktail. (A) Representative images of RBCs mixed with HSA, protein cocktail, and dextran 500 kDa at 100 mg/ml. (B) Aggregation index values determined for blood, sodium chloride (NaCl) solution (i.e., saline), the protein cocktail, HSA, and dextran 500 kDa. Platelet aggregation tests induced with collagen (C) or ADP (D) on the control (saline solution), HSA, Hextend, and the protein cocktail.$^{\dagger}p < .05$ versus no treatment. $^{\ddagger}p < .05$ versus HSA. $^{\S}p < .05$ versus Hextend [Color figure can be viewed at wileyonlinelibrary.com]

mitigate hemolysis-associated toxicity. Moreover, the favorable hemocompatibility, colloidal osmotic pressure (COP), and viscosity properties indicate potentially favorable outcomes in vivo. Indeed, preliminary in vivo studies demonstrated that this protein cocktail could reduce hemolysis-associated iron toxicity.

In addition to the characteristic hemolysis scavenging proteins (Hp, Hpx, and Tf), the protein cocktail contained a large fraction of HSA and other components – Cp and VDB – which may also aid in reducing the toxicity associated with hemolysis. Although not as efficient as either Hpx or Tf, HSA binds to both free heme and free iron, reducing their oxidative toxicity and serving as a reservoir until Hpx and Tf can deliver these molecules to their respective clearance receptors.[32–35] HSA may also serve as a carrier for direct cellular heme or heme-HSA uptake.[36,37] While not a direct scavenger, Cp is a ferroxidase that catalyzes the oxidation of Fe^{2+} into Fe^{3+} and stabilizes ferroportin (cellular iron exporter).[38,39] Notably, the oxidation of iron to Fe^{3+} is required for iron binding to Tf (iron transport) or ferritin (iron storage).[38,40–43] On the other hand, VDB, also known as Gc-globulin, scavenges actin, which is another toxic species released during hemolysis or tissue damage.[44–48]

In addition to directly reducing the toxicity associated with hemolysis, the scavenging protein cocktail has promising biophysical and biochemical properties. Blood viscosity is an important factor that regulates the responses of the cardiovascular system, as it affects shear

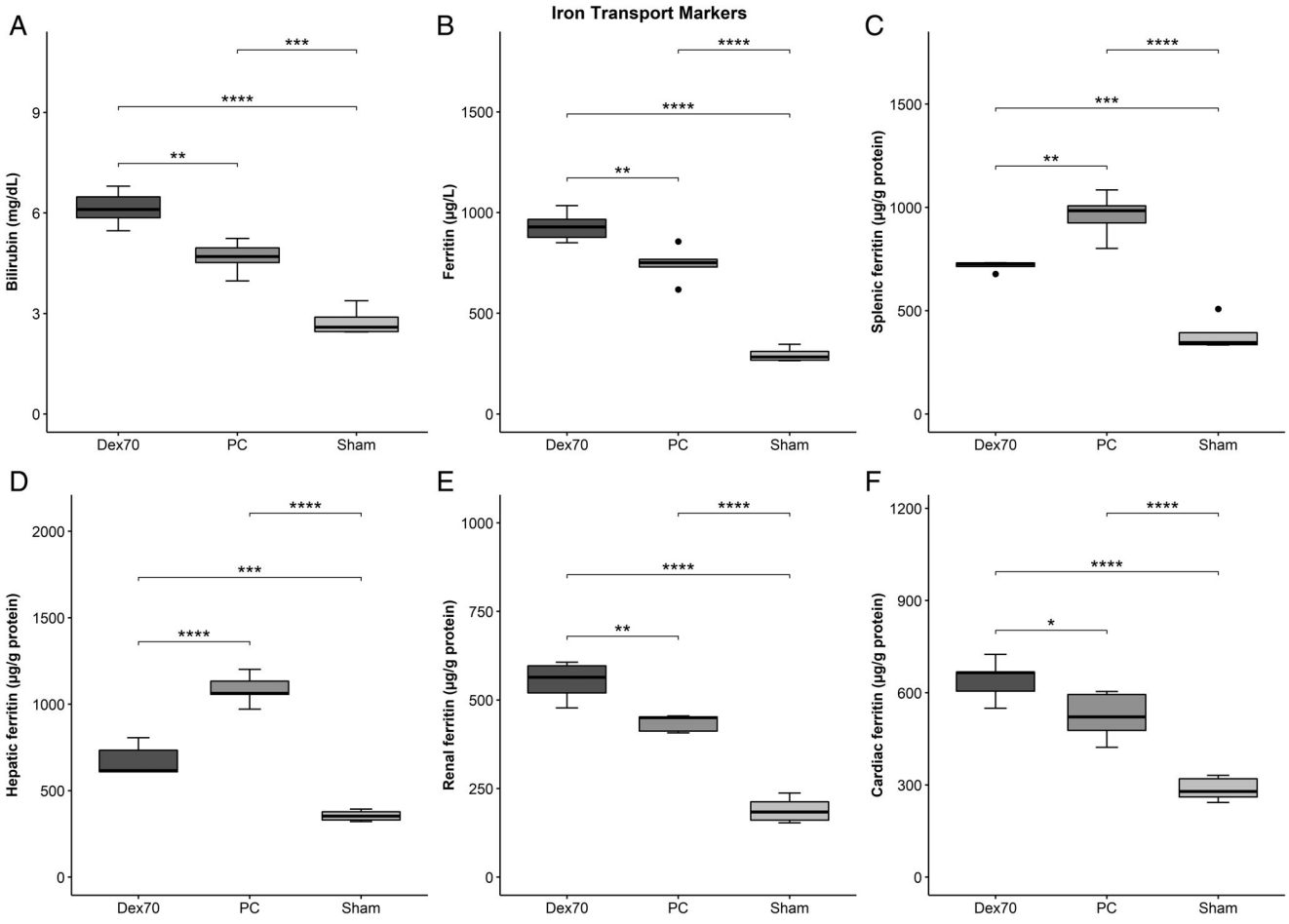

FIGURE 5 Bilirubin and ferritin levels in blood and tissue from animals exchange transfused with mechanically hemolyzed blood plasma mixed with the protein cocktail (PC) or dextran 70 kDa (Dex70). Sham indicates baseline levels in healthy animals. (A) Blood bilirubin, (B) blood ferritin, (C) splenic ferritin, (D) hepatic ferritin, (E) renal ferritin, and (F) cardiac ferritin. Markers measured from hepatic, splenic, renal, and cardiac tissues are normalized to the total protein content in the tissue. N = 5 animals/group. *$p < .05$; **$p < .01$, ***$p < .001$, ****$p < .0001$

stress and activates the synthesis of vascular relaxation mediators such as nitric oxide (NO).[49] NO is a critical regulator of basal blood vessel tone and vascular homeostasis, antiplatelet activity, modulation of endothelial and smooth muscle proliferation, and adhesion molecule expression. However, during states of hemolysis, NO is depleted from the vasculature due to scavenging by cell-free Hb via the NO dioxygenation reaction. However, by using the protein cocktail presented here, the high viscosity of the cocktail could improve shear thinning of RBCs and increase in situ NO production.[50] Moreover, the nonlinear COP of the protein cocktail as a function of protein concentration indicates the potential of the protein cocktail to expand the blood volume beyond the volume infused, which may be used during hypovolemic states. These characteristics may originate from the large MW components of the cocktail, which could promote protein crowding via depletion forces.[51] Furthermore, reduced RBC aggregation maintains the RBC-poor plasma layer near the vascular wall, which positively increases vascular endothelial shear stress. Lastly, the positive hemocompatibility (lack of RBC aggregation) and the preservation of platelet function support the potential application of the protein cocktail for hemolysis mitigation.

Although plasma also contains the same proteins in the protein cocktail, there are safety considerations that favor the use of the processed protein cocktail. Without the presence of immunoglobulins, the protein cocktail serves as a universally transfusable solution. This expands the source of plasma that can be used to purify the protein cocktail, since only 4% of the U.S. population has type AB blood (universal plasma donor).[52] Furthermore, immunoglobulins are known to increase the risk of transfusion-related acute lung injury, which is considered the leading cause of transfusion-related

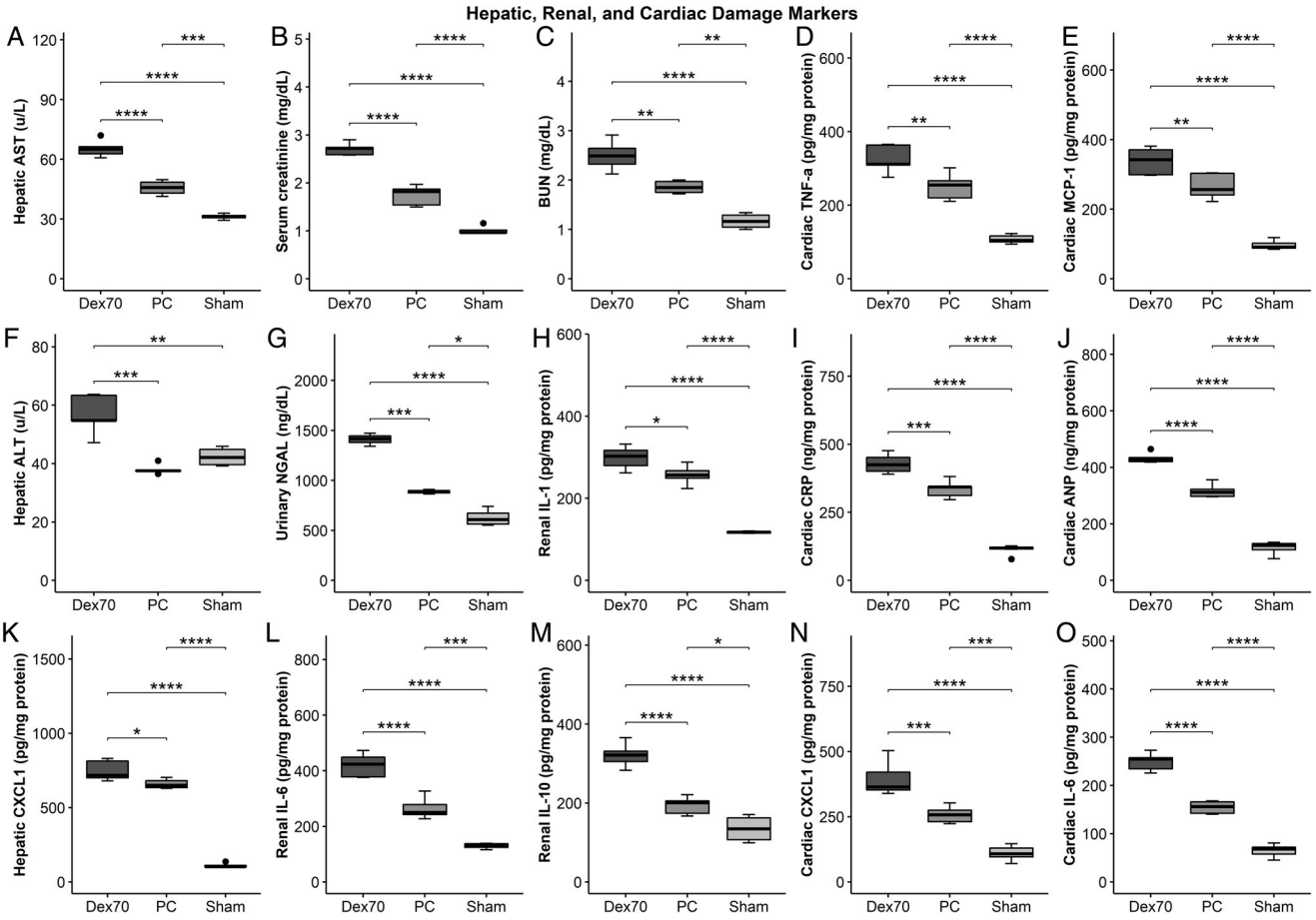

FIGURE 6 Markers of renal, hepatic, and cardiac tissue inflammation and injury from animals exchange transfused with mechanically hemolyzed blood plasma mixed with the protein cocktail (PC) or dextran 70 kDa (Dex70). Sham indicated baseline levels in healthy animals. (A) Hepatic aspartate aminotransferase (AST), (B) serum creatinine, (C) blood urea nitrogen (BUN), (D) cardiac tumor necrosis factor alpha (TNF-α), (E) cardiac monocyte chemoattractant protein-1 (MCP-1), (F) hepatic alanine aminotransferase (ALT), (G) urinary neutrophil gelatinase associated lipocalin (NGAL), (H) renal interleukin-1 (IL-1), (I) cardiac C-reactive protein (CRP), (J) cardiac atrial natriuretic peptide (ANP), (K) hepatic chemokine ligand 1 (CXCL1), (L) renal interleukin-6 (IL-6), (M) renal interleukin-10 (IL-10), (N) cardiac CXCL1, and (O) cardiac IL-6. Markers measured from cardiac, renal and hepatic tissues (i.e., D, E, H, I, J, K, L, M, N, O) are normalized to the total protein content in the tissue. N = 5 animals/group. *$p < .05$; **$p < .01$, ***$p < .001$, ****$p < .0001$

mortality.[53,54] Moreover, due to the ethanol precipitation steps used to produce FIV and the extensive nanofiltration used to isolate the protein cocktail, the risk of transmission of blood-borne infectious agents is greatly minimized compared to plasma administration.

In addition to its improved safety profile, the concentrations of desired hemolysis scavenging proteins in the protein cocktail are enhanced compared to plasma. The protein concentration in human plasma ranges from 60 to 80 mg/ml with a composition of approximately 50% HSA, 5% Tf, 2% Hp, 1% Hpx, and less than 1% of Cp or VDB.[55,56] On the other hand, the concentration of Tf, Hp, Hpx, Cp, and VDB in the protein cocktail was fivefold or greater compared to plasma. Based on the protein composition of the protein cocktail, 500 ml of an iso-oncotic solution (approx. 50–60 mg/ml) could scavenge and detoxify approximately 3% of the total Hb, >6% of the total heme, and > 6% of the total iron contained in a packed RBC unit. Therefore, this composition would be more than sufficient to neutralize the hemolysis byproducts derived from the 1% ex vivo hemolysis limit set by the U.S. Food and Drug Administration for a unit of blood, and the high Tf content could potentially prevent build-up of non-transferrin bound iron after catabolism of RBCs.[57] Moreover, both Hpx and Tf may be recycled after receptor-mediated uptake in vivo, enabling the contents of the cocktail to detoxify/neutralize more hemolytic species than estimated.[58,59]

Future generations of the protein cocktail may have altered composition by supplementing with additional

proteins or adding additional processing steps before or after the filtration system presented here such as precipitation with ammonium sulfate or chromatographic techniques.[60] However, these extra processing steps would increase manufacturing costs and complexity.

5 | CONCLUSIONS

Approximately 60 g of a protein cocktail was isolated from 500 g of FIV via TFF, yielding a protein mixture with Hb-, heme-, and iron-binding capability. Interestingly, the protein cocktail showed a nonlinear concentration dependence with respect to viscosity and COP, which are advantageous properties for NO regulation and plasma expansion. Furthermore, the protein cocktail did not elicit red blood cell aggregation nor inhibit platelet aggregation in vitro. The reduction of hemolysis-mediated toxicity was confirmed in vivo where animals treated with the protein cocktail had improved iron transport and reduced damage in cardiac, hepatic, and renal tissues.

Taken together, this study presents a simple and effective method to purify and characterize a blood-compatible protein cocktail capable of scavenging free iron, free heme, and cell-free Hb for possible treatment of states of hemolysis. Future studies will further characterize the in vivo efficacy of this protein cocktail in mitigating hemolysis-mediated toxicity and potentially optimize the protein composition of the mixture for target indications.

ACKNOWLEDGMENT

We acknowledge Mani Grevenow (Transfusion Services, Wexner Medical Center, The Ohio State University) for generously donating expired human RBC units. This work was supported by National Institutes of Health grants R01HL126945, R01EB021926, and R01HL138116, the Ohio State University Office of Undergraduate Research & Creative Inquiry Summer Research Fellowship, and the Pelotonia Fellowship Program. The project was also supported by NIH grant P30 CA016058. The Fusion Orbitrap instrument was supported by NIH grant S10 OD018056. Any opinions, findings, and conclusions expressed in this material are those of the author(s) and do not necessarily reflect those of the Pelotonia Fellowship Program.

AUTHOR CONTRIBUTIONS

The manuscript was written through the contributions of all authors. All authors have given approval to the final version of the manuscript.

CONFLICT OF INTEREST

ISP and AFP are inventors on pending patent applications outlining methods related to protein purification and their uses (PCT/US2020/016267 and PCT/US2021/023441). PC is a co-inventor on PCT/US2021/023441.

ORCID

Ivan S. Pires https://orcid.org/0000-0002-4035-0027
Krianthan Govender https://orcid.org/0000-0002-8632-6452
Carlos J. Munoz https://orcid.org/0000-0003-4832-3661
Quintin T. O'Boyle https://orcid.org/0000-0003-1499-9620
Chintan Savla https://orcid.org/0000-0001-7538-8861
Pedro Cabrales https://orcid.org/0000-0002-8794-2839

REFERENCES

1. Buehler PW, Karnaukhova E. When might transferrin, hemopexin or haptoglobin administration be of benefit following the transfusion of red blood cells? Curr Opin Hematol. 2018;25:452–8.
2. Schaer DJ, Buehler PW, Alayash AI, Belcher JD, Vercellotti GM. Hemolysis and free hemoglobin revisited: Exploring hemoglobin and hemin scavengers as a novel class of therapeutic proteins. Blood. 2013;121:1276–84.
3. Boretti FS, Buehler PW, D'Agnillo F, Kluge K, Glaus T, Butt OI, et al. Sequestration of extracellular hemoglobin within a haptoglobin complex decreases its hypertensive and oxidative effects in dogs and Guinea pigs. J Clin Invest. 2009;119:2271–80.
4. Pires IS, Savla C, Palmer AF. Poly(ethylene glycol) surface-conjugated apohemoglobin as a synthetic heme scavenger. Biomacromolecules. 2020;21:2155–64.
5. Eaton JW, Qian M. Molecular bases of cellular iron toxicity. Free Radic Biol Med. 2002;32:833–40.
6. Fraga CG, Oteiza PI. Iron toxicity and antioxidant nutrients. Toxicology. 2002;180:23–32.
7. Brissot P, Ropert M, Le Lan C, Loréal O. Non-transferrin bound iron: A key role in iron overload and iron toxicity. Biochim Biophys Acta. 2012;1820:403–10.
8. Deuel JW, Schaer CA, Boretti FS, Opitz L, Garcia-Rubio I, Baek JH, et al. Hemoglobinuria-related acute kidney injury is driven by intrarenal oxidative reactions triggering a heme toxicity response. Cell Death Dis. 2016;7:e2064.
9. Rother RP, Bell L, Hillmen P, Gladwin MT. The clinical sequelae of intravascular hemolysis and extracellular plasma hemoglobin: A novel mechanism of human disease. JAMA. 2005;293:1653–62.
10. Schaer DJ, Vinchi F, Ingoglia G, Tolosano E, Buehler PW. Haptoglobin, hemopexin, and related defense pathways - Basic science, clinical perspectives, and drug development. Front Physiol. 2014;5:415.
11. Remy KE, Cortés-Puch I, Solomon SB, Sun J, Pockros BM, Feng J, et al. Haptoglobin improves shock, lung injury, and survival in canine pneumonia. JCI Insight. 2018;3:e123013.
12. Graw JA, Mayeur C, Rosales I, Liu Y, Sabbisetti VS, Riley FE, et al. Haptoglobin or hemopexin therapy prevents acute adverse effects of resuscitation after prolonged storage of red cells. Circulation. 2016;134:945–60.

13. Baek JH, Yalamanoglu A, Gao Y, Guenster R, Spahn DR, Schaer DJ, et al. Iron accelerates hemoglobin oxidation increasing mortality in vascular diseased Guinea pigs following transfusion of stored blood. JCI Insight. 2017;2:e93577.
14. Munoz CJ, Pires IS, Baek JH, Buehler PW, Palmer AF, Cabrales P. Apohemoglobin-haptoglobin complex attenuates the pathobiology of circulating acellular hemoglobin and heme. Am J Physiol Circ Physiol. 2020;318:H1296–307.
15. Belcher DA, Munoz C, Pires IS, Williams AT, Cabrales P, Palmer AF. Apohemoglobin-haptoglobin complexes attenuate the hypertensive response to low-molecular-weight polymerized hemoglobin. Blood Adv. 2020;4:2739–50.
16. Chen-Roetling J, Ma S-K, Cao Y, Shah A, Regan RF. Hemopexin increases the neurotoxicity of hemoglobin when haptoglobin is absent. J Neurochem. 2018;145:464–73.
17. Montecinos L, Eskew JD, Smith A. What is next in this "Age" of heme-driven pathology and protection by hemopexin? An update and links with iron. Pharmaceuticals. 2019;12:144.
18. Pires IS, Palmer AF. Tangential flow filtration of haptoglobin. Biotechnol Prog. 2020;36:e3010.
19. Winterbourn CC. Oxidative reactions of hemoglobin. Methods Enzymol. 1990;186:265–72.
20. Pires IS, Belcher DA, Hickey R, Miller C, Badu-Tawiah AK, Baek JH, et al. Novel manufacturing method for producing apohemoglobin and its biophysical properties. Biotechnol Bioeng. 2020;117:125–45.
21. Frieden E, Aisen P. Forms of iron transferrin. Trends Biochem Sci. 1980;5:10.
22. Meng F, Alayash AI. Determination of extinction coefficients of human hemoglobin in various redox states. Anal Biochem. 2017;521:11–9.
23. Pires IS, Belcher DA, Palmer AF. Quantification of active apohemoglobin heme-binding sites via dicyanohemin incorporation. Biochemistry. 2017;56:5245–59.
24. Gentinetta, T., Brinkman, N., Boerema, D., An, B. & Miner, K. Hemopexin formulations. (2019). Available from: https://patentscope.wipo.int/search/en/detail.jsf;jsessionid=B7BF8060CF2FA0F81341CEB8D601FD8F.wapp1nC?docId=WO2019030262&tab=PCTDOCUMENTS.
25. Elmer J, Cabrales P, Wang Q, Zhang N, Palmer AF. Synthesis and biophysical properties of polymerized human serum albumin. Biotechnol Prog. 2011;27:290–6.
26. Lee BK, Alexy T, Wenby RB, Meiselman HJ. Red blood cell aggregation quantitated via myrenne aggregometer and yield shear stress. Biorheology. 2007;44:29–35.
27. Oronsky B, Oronsky N, Cabrales P. Platelet inhibitory effects of the phase 3 anticancer and normal tissue cytoprotective agent, RRx-001. J Cell Mol Med. 2018;22:5076–82.
28. Muller CR, Williams AT, Munoz CJ, Eaker AM, Breton AN, Palmer AF, et al. Safety profile of high molecular weight polymerized hemoglobins. Transfusion. 2021;61:212–24.
29. Hortin GL, Remaley AT. Mass determination of major plasma proteins by matrix-assisted laser desorption/ionization time-of-flight mass spectrometry. Clin Proteomics. 2006;2:103–16.
30. Gombocz K, Beledi Á, Alotti N, Kecskés G, Gábor V, Bogár L, et al. Influence of dextran-70 on systemic inflammatory response and myocardial ischaemia-reperfusion following cardiac operations. Crit Care. 2007;11:R87.
31. Barbu M, Kolsrud O, Ricksten S-E, Dellgren G, Zetterberg H, Blennow K, et al. Dextran- versus crystalloid-based prime in cardiac surgery: A prospective randomized pilot study. Ann Thorac Surg. 2020;110:1541–7.
32. Loban A, Kime R, Powers H. Iron-binding antioxidant potential of plasma albumin. Clin Sci (Lond). 1997;93(445–51):445–51.
33. Taverna M, Marie A-L, Mira J-P, Guidet B. Specific antioxidant properties of human serum albumin. Ann Intensive Care. 2013;3:4.
34. Tolosano E, Altruda F. Hemopexin: Structure, function, and regulation. DNA Cell Biol. 2002;21:297–306.
35. Smith A, McCulloh RJ. Hemopexin and haptoglobin: Allies against heme toxicity from hemoglobin not contenders. Front Physiol. 2015;6:187.
36. Jennifer B, Berg V, Modak M, Puck A, Seyerl-Jiresch M, Künig S, et al. Transferrin receptor 1 is a cellular receptor for human heme-albumin. Commun Biol. 2020;3:621.
37. Noyer CM, Immenschuh S, Liem HH, Muller-Eberhard U, Wolkoff AW. Initial heme uptake from albumin by short-term cultured rat hepatocytes is mediated by a transport mechanism differing from that of other organic anions. Hepatology. 1998;28:150–5.
38. Ramos D, Mar D, Ishida M, Vargas R, Gaite M, Montgomery A, et al. Mechanism of copper uptake from blood plasma ceruloplasmin by mammalian cells. PLoS One. 2016;11:e0149516.
39. De Domenico I, Ward DM, di Patti MCB, Jeong SY, David S, Musci G, et al. Ferroxidase activity is required for the stability of cell surface ferroportin in cells expressing GPI-ceruloplasmin. EMBO J. 2007;26:2823–31.
40. de Silva D, Aust SD. Stoichiometry of Fe(II) oxidation during ceruloplasmin-catalyzed loading of ferritin. Arch Biochem Biophys. 1992;298:259–64.
41. Samokyszyn VM, Miller DM, Reif DW, Aust SD. Inhibition of superoxide and ferritin-dependent lipid peroxidation by ceruloplasmin. J Biol Chem. 1989;264:21–6.
42. de Silva DM, Aust SD. Ferritin and ceruloplasmin in oxidative damage: Review and recent findings. Can J Physiol Pharmacol. 1993;71:715–20.
43. Hellman NE, Gitlin JD. Ceruloplasmin metabolism and function. Annu Rev Nutr. 2002;22:439–58.
44. Smith D, Janmey P, Sherwood J, Howard R, Lind S. Decreased plasma gelsolin levels in patients with *Plasmodium falciparum* malaria: A consequence of hemolysis? Blood. 1988;72:214–8.
45. Peddada N, Sagar A, Garg R. Plasma gelsolin: A general prognostic marker of health. Med Hypotheses. 2012;78:203–10.
46. Piktel E, Levental I, Durnaś B, Janmey P, Bucki R. Plasma gelsolin: Indicator of inflammation and its potential as a diagnostic tool and therapeutic target. Int J Mol Sci. 2018;19:2516.
47. Meier U, Gressner O, Lammert F, Gressner AM. Gc-globulin: Roles in response to injury. Clin Chem. 2006;52:1247–53.
48. Chun RF. New perspectives on the vitamin D binding protein. Cell Biochem Funct. 2012;30:445–56.
49. Tsai AG, Acero C, Nance PR, Cabrales P, Frangos JA, Buerk DG, et al. Elevated plasma viscosity in extreme hemodilution increases perivascular nitric oxide concentration and microvascular perfusion. Am J Physiol Circ Physiol. 2005;288:H1730–9.

50. Meng F, Kaul D, Thangaswamy S, Bhutoria S, Gerfen G, Branch C, et al. Semisynthetic supra plasma expanders: A new class of therapeutics to improve microcircualtion in sickle cell anaemia. Artif Cells Nanomed Biotechnol. 2019;47: 73–82.
51. Mitchison TJ. Colloid osmotic parameterization and measurement of subcellular crowding. Mol Biol Cell. 2019;30: 173–80.
52. Nascimento B, Callum J, Rubenfeld G, Neto J, Lin Y, Rizoli S. Clinical review: Fresh frozen plasma in massive bleedings - More questions than answers. Crit Care. 2010;14:202.
53. Kim J, Na S. Transfusion-related acute lung injury; clinical perspectives. Korean J Anesthesiol. 2015;68:101–5.
54. Miller TE. New evidence in trauma resuscitation - Is 1:1:1 the answer? Perioper Med. 2013;2:13.
55. Li C, Tan XF, Lim TK, Lin Q, Gong Z. Comprehensive and quantitative proteomic analyses of zebrafish plasma reveals conserved protein profiles between genders and between zebrafish and human. Sci Rep. 2016;6:24329.
56. Kramer G, Woolerton Y, van Straalen JP, Vissers JPC, Dekker N, Langridge JI, et al. Accuracy and reproducibility in quantification of plasma protein concentrations by mass spectrometry without the use of isotopic standards. PLoS One. 2015;10:e0140097.
57. Rapido F, Brittenham GM, Bandyopadhyay S, La Carpia F, L'Acqua C, McMahon DJ, et al. Prolonged red cell storage before transfusion increases extravascular hemolysis. J Clin Invest. 2017;127:375–82.
58. Smith A. Protection against heme toxicity: Hemopexin rules, OK? Ferreira G. C., Kadish K. M., Smith K. M., Guilard R., Handbook of porphyrin science; 30 5 Toh Tuck Link, Singapore 596224: World Scientific Publishing Co Pte Ltd; 2013. p. 311–38. https://doi.org/10.1142/9789814407755_0045.
59. Mayle KM, Le AM, Kamei DT. The intracellular trafficking pathway of transferrin. Biochim Biophys Acta. 2012;1820:264–81.
60. Raoufinia R, Mota A, Keyhanvar N, Safari F, Shamekhi S, Abdolalizadeh J. Overview of albumin and its purification methods. Adv Pharm Bull. 2016;6:495–507.

SUPPORTING INFORMATION

Additional supporting information may be found online in the Supporting Information section at the end of this article.

How to cite this article: Pires IS, Govender K, Munoz CJ, et al. Purification and analysis of a protein cocktail capable of scavenging cell-free hemoglobin, heme, and iron. *Transfusion*. 2021; 1–14. https://doi.org/10.1111/trf.16393